

Article

A Novel MPPT Controller Based on Mud Ring Optimization Algorithm for Centralized Thermoelectric Generator under Dynamic Thermal Gradients

Muhammad Hamza Zafar ¹, Mohamad Abou Houran ² , Majad Mansoor ³, Noman Mujeeb Khan ⁴,
Syed Kumayl Raza Moosavi ⁵, Muhammad Kamran Khan ⁶ and Naureen Akhtar ^{7,*}

- ¹ Department of Electrical Engineering, Capital University of Science and Technology, Islamabad 44000, Pakistan
- ² School of Electrical Engineering, Xi'an Jiaotong University, No. 28, West Xianning Road, Xi'an 710049, China
- ³ Department of Automation, University of Science and Technology of China, Hefei 230027, China
- ⁴ Department of Electrical Engineering, Beaconhouse International College, Islamabad 44000, Pakistan
- ⁵ School of Electrical and Electronics Engineering, National University of Sciences and Technology, Islamabad 44000, Pakistan
- ⁶ Islamabad Campus, Hamdard University, Islamabad 44000, Pakistan
- ⁷ Department of Engineering Sciences, University of Agder, 4876 Grimstad, Norway
- * Correspondence: naureen.akhtar@uia.no

Abstract: Most industrial processes generate raw heat. To enhance the efficiency of industrial operations, this raw heat is recovered. Thermoelectric generators (TEG), as solid state devices, provide an excellent application of heat recovery in the form of most manageable electrical power. This work presents a novel MPPT controller based on the Mud Ring Optimization algorithm for a centralized Thermoelectric Generator (TEG) under dynamic thermal gradients. The existing stochastic optimization algorithm for Maximum Power Point Tracking (MPPT) control in renewable energy systems exhibits several limitations that affect its performance in MPPT control. The convergence speed, local minima trap, hyper parameters' sensitivity toward the population size, acceleration coefficients, and the stopping criterion all impact the convergence stability. In addition to these limitations, sensor noise sensitivity in measurement fluctuates the control system leading to reduced performance. Therefore, the careful design and implementation of the MRO algorithm is crucial to overcome these limitations and achieve a satisfactory performance in MPPT control. The results of this study contribute to developing more efficient MPPT control of TEG systems and implementing renewable energy technologies. The algorithm effectively tracks the maximum power point in dynamic thermal environments and increases the power output compared to conventional MPPT methods. The findings illustrate the efficacy of the proposed controller providing a higher power output (Avg. 99.95%) and faster response time (220 ms) under dynamic thermal conditions achieving 38–70% faster tracking of the GM in dynamic operating conditions.

Keywords: mud ring algorithm; power extraction; heat recovery; swarm intelligence; thermoelectric generation



Citation: Zafar, M.H.; Abou Houran, M.; Mansoor, M.; Khan, N.M.; Moosavi, S.K.R.; Khan, M.K.; Akhtar, N. A Novel MPPT Controller Based on Mud Ring Optimization Algorithm for Centralized Thermoelectric Generator under Dynamic Thermal Gradients. *Appl. Sci.* **2023**, *13*, 4213. <https://doi.org/10.3390/app13074213>

Academic Editor: Gang Lei

Received: 3 February 2023

Revised: 5 March 2023

Accepted: 24 March 2023

Published: 26 March 2023



Copyright: © 2023 by the authors. Licensee MDPI, Basel, Switzerland. This article is an open access article distributed under the terms and conditions of the Creative Commons Attribution (CC BY) license (<https://creativecommons.org/licenses/by/4.0/>).

1. Introduction

The Seebeck effect allows solid-state thermoelectric generators (TEG) to convert heat into electricity. They have several advantages over traditional generators, such as high efficiency, low maintenance, and the ability to operate in extreme environments. However, one of the challenges in using TEGs is maximizing the power delivered to the load. In a TEG system, the power output rests on the temperature gradient across the device and the thermal resistance. Non-uniform temperature distribution in the system can significantly affect the power output, leading to a decrease in the productivity of the system.

Therefore, it is important to accurately track the maximum power point to optimize the TEG's performance.

There have been several MPPT control techniques proposed in the literature to address this issue. One commonly used method is the perturb and observe (P&O) algorithm, which adjusts the operating point of the TEG in small increments and compares the power output to determine the maximum power point. However, the P&O algorithm can be slow and may not always converge to the optimal solution. Other methods, such as fuzzy logic and artificial-neural-network-based approaches, have been proposed to improve the convergence speed and accuracy of the MPPT process.

Recently, metaheuristic algorithms have gained popularity for use in the MPPT control of TEG systems. Metaheuristic algorithms are optimization techniques that mimic the behavior of natural systems and can find near-optimal solutions to complex problems. They have the advantage of being able to handle the constraints and uncertainties present in real-world systems. Examples of metaheuristic algorithms that have been applied to TEG MPPT include particle swarm optimization (PSO), genetic algorithms (GA), and ant colony optimization (ACO).

This work deals with complications generated by non-uniform temperature distribution across TEG module arrays connected in centralized control topology. The performance of the proposed algorithm is compared to other commonly used MPPT control techniques, including P&O, fuzzy logic, and artificial neural networks. The results show that the proposed algorithm can achieve faster convergence and higher efficiency compared to the other methods.

Overall, the use of metaheuristic algorithms in the MPPT control of TEG systems has the potential to improve the efficiency and performance of these devices, causing them to be a viable alternative to traditional generators in a variety of applications.

1.1. Literature

In the literature, several aspects of TEG systems have been studied. Smart Maximum Power Point Tracking (MPPT) is essential for optimizing the performance of renewable energy systems thermoelectric (TEG). Using TEG systems as a heat recovery unit with smart MPPT control is shown in Figure 1. The TEG modules are exposed to the hot surface, and the temperature differential across the TEG module, using the Peltier's and Seebeck's effect, generates the voltage potential that is modulated using the DC boost converter via the PWM signal generated by the MPPT controller under conditions provided by the current and voltage sensors [1]. Figure 2 shows the internal structure and electrical equivalent model. Figure 3 shows one of the most cost-effective topologies of TEG system to act as a heat recovery system. The electrical characteristics exhibited in Figure 4 show that the control problem in hand is not only nonlinear but also mathematically monotonic and multiple maxima [2]. MPPT is used to track the maximum power point of the TEG and to ensure that the TEG operates at its maximum power output. This is important in TEG systems that are used for heat recovery applications, where the TEG converts waste heat into electrical energy.

The classical MPPT techniques that have been developed for TEG systems include perturb and observe (P&O), incremental conductance (IC) in fusion with fuzzy logic control (FLC), machine learning (ML) models, and deep neural networks (DNN). Unlike PV and wind energy conversion systems, these techniques are less explored in TEG systems. The P&O technique is a simple and widely used MPPT technique that adjusts the TEG's operating voltage in fixed magnitude in forward or reverse depending upon the change in output power. Since the decisions are made due to the gradient ascend or descend in the presence multiple local peak solution (shown in Figure 4), the MPPT control, hence, may trap in local maxima, thus losing significant available power. The IC technique is similar to the P&O technique, but it uses a conductance parameter, which is a more sophisticated control algorithm to adjust the TEG's operating voltage.

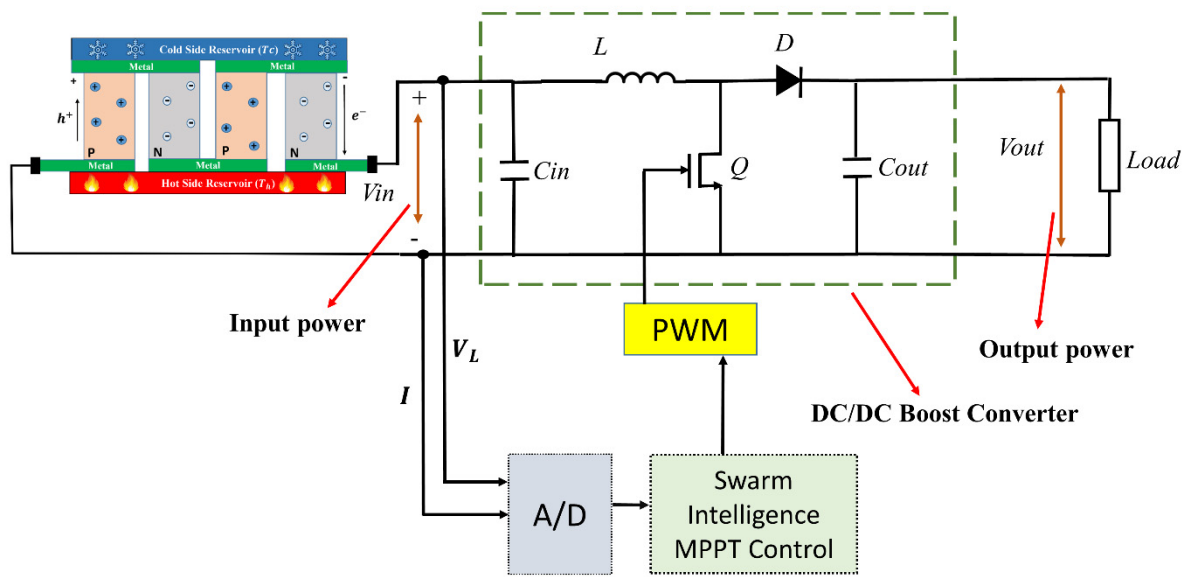


Figure 1. TEG system with MPPT.

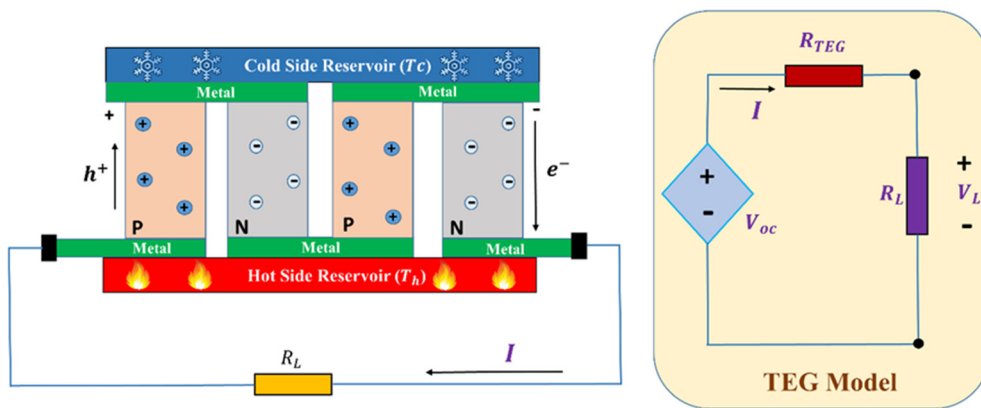


Figure 2. TEG module structure with equivalent electrical circuit.

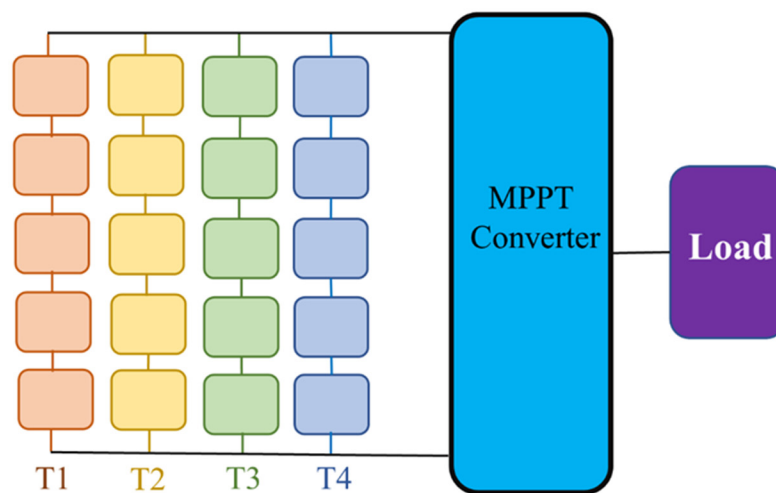


Figure 3. Centralized TEG configuration with load and MPPT converter.

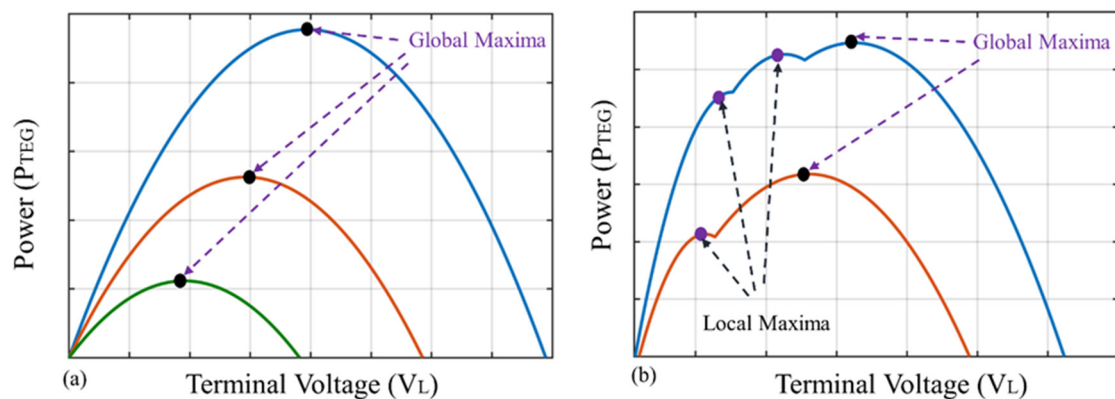


Figure 4. P–V curve of TEG modules under (a) uniform temperature and (b) non-uniform temperature.

In recent years, there has been a growing interest in the development of novel MPPT techniques for TEG systems. These optimization algorithms have been shown to be effective in improving the performance of TEG systems by providing a more accurate and efficient method for tracking the maximum power point.

The study found that the PSO algorithm was able to track the maximum power point more accurately and quickly, leading to a higher power output and better energy harvesting. MPPT may be thought of as an optimization issue. Swarm-intelligence-based optimization techniques and other meta-heuristic evolutionary algorithms have a great deal of potential to overcome the drawbacks of FLC, ML, and traditional MPPT methods [3]. The FLC technique uses fuzzy logic to determine the TEG’s operating voltage, which is then adjusted to track the maximum power point. The nonlinear multiplicity of the base system’s less precise equivalent modeling can be handled by the SI with ease. For PSO and for MPPT in TEG systems, [4] found that the PSO algorithm was able to significantly improve the efficiency of the TEG system, compared to other MPPT techniques, such as P&O. In this class, particle swarm optimization (PSO) [5,6], grey wolf optimization (GWO) [7], Harris hawk optimization (HHO) [8], grasshopper optimization (GHO) [9], and ant colony optimization (ACO) [10,11] are most implemented techniques. The simulated annealing (SA) performance in [12] is assessed by considering the converge time and the number of samples to converges to the GMPP. A cuckoo search (CS) algorithm has variants that generate the searching pattern using the Levy Flight Functions (LFF) as in [13,14]. LFF generate sharp large fluctuations that equate the voltage surges in the DC Boost converters. The overall distribution (OD) algorithm in [15] is fused with PSO for rapid convergence time. The adaptive cuckoo optimization algorithm (ACOA) [16] minimizes the LFF impact in an iterative manner to avoid the voltage surges and increase the convergence time. The farmland fertility optimization (FFO) [17], spline-guided Jaya (SGJ) algorithm [18], salp swarm optimization algorithm (SSA) [19], and Butterfly optimization algorithm (BOA) [20] work in a similar manner using dynamic variables to control the balance between the exploitation and exploration phases of the GMPP-searching mechanisms. The artificial bee colony (ABC) [21] used dynamic association of searching members and scout members to achieve the GMPP and avoid the LM traps. To minimize the impact of random vectors in a standard PSO, an improvised one is modeled using the particle swarm optimization gravitational search (PSOGS). In these algorithms, the population size, information exchange mechanisms, number of epochs and iterations, convergence rates, parametric tuning, and computation burden are just a few examples of the variables that affect the SI performance [22].

Another recent study that used GAs for MPPT in TEG systems found that the GA algorithm was able to improve the performance of the TEG system, compared to other MPPT techniques, such as P&O and IC.

A random number will produce unexpected oscillation and affect the stability time of the particle swarm optimization algorithm [18]. PSOGS combines the effective exploration of PSO with the precise development of GS, which greatly improves the work efficiency of PSO. Even though the steady-state oscillation has improved, the stabilization time has not been greatly reduced. The number of parameters that must be adjusted, the level of technical difficulty, and the computational load all rise as a result of the combination of GS and PSO. By using the arithmetic optimization method (AOA) [23], the random and adaptive parameter selection principle greatly boosts the AOA convergence performance. ACO uses pheromones to share information. Pheromones evaporate over time. Each ant is a member of a collection of possible solutions. Scout ants are also used to explore the search space [24]. Due to the selection of candidate solutions using probability functions, the undesired solution is selected for the output. The fitness-dependent algorithm (FDO) [25] and ABC mimic bee behavior. The pheromone evaporation rate yields solution degradation causing defective final solutions. Similarly, in CSA, Levy flight is used to allocate burst random values, which will lead to large fluctuations in the output transients [13]. The study found that the GA algorithm was able to track the maximum power point more accurately, leading to a higher power output and better energy harvesting. In a small size population, shortcomings such as oscillations and fluctuations predominate [26]. To smoothen the oscillations and enhance stability, a larger number of search agents is recommended. Consequently, the computing power is affected by exponential and convergence time delays. The main objectives required from the MPPT techniques are GM detection, robustness, fast convergence, least random oscillation, and high power convergence [27]. Thus, the maximum available energy is delivered to the load. Although GHO, CSA, ACO, etc., exhibit a reasonable power tracking ability, the logical flow of these algorithms contains randomness and is more complicated than the traditional PSO algorithm, which causes their actual implementation to be challenging in low-cost MPPT control [28,29].

In conclusion, the literature review indicates that there is a growing body of research on the development of MPPT techniques for TEG systems, particularly in the area of optimization algorithms, such as gradient-based algorithms (P&O, IC), evolutionary algorithms (GA, DE, SA), and nature-inspired metaheuristics algorithms (PSO, GWO). These optimization algorithms have been shown to be effective in improving the performance of TEG systems, by providing a more accurate and efficient method for tracking the maximum power point. However, each class comes with some limitations to it. Further research is needed to develop and validate these MPPT techniques for TEG systems, particularly in the context of heat-recovery applications. The main contributions of the presented work are summarized as:

- A novel mud-ring-optimizer-based MPPT control technique is implemented and tested on dynamic non-uniform thermal gradients.
- The proposed MRA-based MPPT technique can track the GMPP under non-uniform temperature distribution with 99.96% efficiency within 220 ms.
- The comparison of the MRA-based technique is performed with WOA-, GWO-, and PSO-based state-of-the-art MPPT techniques.
- The MRA-based technique has a strong capability to differentiate between the LMPP and GMPP.
- The proposed technique is also tested using an experimental setup by implementing the proposed technique on a low-cost microcontroller.
- During the experimental verification, the proposed technique achieved a higher efficiency and required less time to track the GMPP.

1.2. TEG Modeling

The thermoelectric generation building block consists of thermocouples that are connected in a series configuration. The main objective of the thermoelectric generator is to convert the thermal energy to electrical energy based on the Seebeck effect, i.e., the

temperature difference at the junctions between two different metals results in a voltage. The TEG module structure with an equivalent electrical circuit is shown in Figure 2. The electrical equivalent of a thermoelectric generator consists of a voltage source with its internal resistance. If the difference in the temperature between the hot and cold junctions is constant, the open circuit voltage of a particular module is provided as follows:

$$V_{TEG} = s_{p-n} \Delta T = s_{p-n} (T_h - T_c) \quad (1)$$

where V_{TEG} is the open circuit voltage, s_{p-n} is the Seebeck co-efficient, and ΔT is the variation in temperature between the hot junction T_h and the cold junction T_c . The Seebeck co-efficient depends upon the type of material used for TEG. The Seebeck coefficient can be determined as follows:

$$s_{p-n} = n_t (s_p - s_n) \quad (2)$$

where n_t are the number of thermocouples, and s_p and s_n indicate the Seebeck co-efficient for p-type and n-type thermocouples. The voltage, current, and output power of the thermoelectric generator can be mathematically expressed as:

$$V_{TEG} = \left(\frac{(s_p - s_n) \times (T_h - T_c) \times r_L}{r_L - r_{TEG}} \right) \times n_t \quad (3)$$

$$I = \frac{(s_p - s_n) \times (T_h - T_c)}{r_L - r_{TEG}} \quad (4)$$

$$P_{TEG} = r_L \times \frac{(s_p - s_n)^2 \times (T_h - T_c)^2}{(r_L - r_{TEG})^2} \times n_t \quad (5)$$

where r_L represents the load resistance in Ω and r_{TEG} represents the internal resistance of TEG. The currently studied TEG model is rated at 25 W with 40 mm \times 40 mm based on Bi2Te3 material. The used centralized TEG structure is shown in Figure 3 and the IV and PV curve under uniform and non-uniform temperature distribution is shown in Figure 4.

The MPP of a TEG system is the operating point at which the generator can produce the maximum amount of power for a given temperature gradient. The accurate tracking of the MPP is critical for achieving the maximum efficiency and performance of the TEG system. If the TEG system is not able to accurately track the MPP, the generator may not be able to operate at its maximum power output, thus resulting in reduced efficiency and performance. Furthermore, TEG systems often have non-uniform temperature gradients due to various factors such as uneven heating or cooling, variations in material properties, and environmental conditions. These non-uniform temperature gradients can significantly affect the accuracy of the MPP tracking in the TEG system. If the MPP tracking is not accurate in a TEG system with non-uniform temperature gradients, it can lead to inefficient energy conversion and reduced power output. Therefore, it is essential to accurately track the MPP in a TEG system, especially when there are non-uniform temperature gradients present. This can be achieved by using advanced control algorithms and feedback mechanisms that can adjust the TEG system's operating conditions in real-time to maintain the system at its MPP. Accurate MPP tracking in TEG systems with non-uniform temperature gradients can result in improved efficiency, increased power output, and reduced energy waste, causing TEG systems to be a more viable and sustainable option for energy conversion.

2. Mud Ring Optimization Algorithm

Bottlenose dolphins collaborate by working together to maximize the hunting effort to obtain food. Dolphins employ a variety of hunting techniques. These approaches change depending on the prey and surrounding circumstances (habitat). Mud Ring feeding, also known as mud plume fishing, is a distinctive foraging technique that was discovered for the first time in 1999 as researchers were observing bottlenose dolphins' behavior in the

shallow waters near Florida’s Atlantic coast. In this style of foraging, the dolphins form a swarm and then one dolphin from the swarm swims in a circle around the prey (a group of fish), swinging its tail up and down along the sand to generate a ring or plume of mud that throws the fish off balance.

The Mud Ring Algorithm (MRA) mimics this bottlenose dolphin foraging behavior, commencing with the echolocation-based food search and concluding with the formation of a mud ring for eating. The MRA behavior is established for the optimum way of obtaining a target as a mathematical simulation. The K parameter is the core of the optimization algorithm process since it illustrates how the dolphin swarm moves closer to the target each time the hunting process begins. This parameter regulates the changeover between the stages of exploring for prey (exploration) and exploitation (mud ring) by reducing the sound volume each time the swarm approaches the prey.

2.1. Mathematical Model

This subsection presents a mathematical simulation of mud ring feeding and hunting for food. The Mud Ring Algorithm (MRA) phases may be described as the following.

2.1.1. Foraging—Exploration Phase: Echolocation

This involves randomly employing dolphins with different exploration velocities (V) at places DE and a kinetic energy (K) that does not produce the sound to alert potential prey. The echolocation also employs sound, but it varied under several factors. The supposition is that the pulse rate ‘ r ’ changes over time, ranging from 0 to 1, where 0 represents no pulse emission and 1 represents the maximum emission rate. Dolphins can adapt the volume of their sounds according to the proximity of their prey, automatically adjusting. The vector K ’s computations are as follows:

$$K = 2a \cdot r - a \tag{6}$$

$$a = 2 \left(1 - \frac{C_{iter}}{Max_{iter}} \right) \tag{7}$$

Generic solutions are used to explore (hunt prey) in a d -dimensional parameter space dictated by the proximity. K is employed to cause divergence and search for the optimal prey, changing randomly with values >1 or <1 . As a result, a dolphin picked at random is chosen rather than the best dolphin. This mechanism allows for a detailed search for the optimum solution. The standards for updating the locations and velocities must be provided. According to the velocity VE_t at time step t , the workability $D(t)$ is supplied by:

$$D(t) = D(t - 1) + V \tag{8}$$

where a random vector V is used as its initial state. According to the magnitude of the target issue, a random velocity from the range $[V_{min}, V_{max}]$ is initially assigned to each dolphin.

2.1.2. Mud Ring Feed—Phase: Exploitation

Dolphins locate and encircle their prey after detection. Since the optimal design position in the search space is unknown beforehand, the MRA uses the closest or optimal prey as the current best solution. The best search agent is selected, and the other dolphins accordingly adjust their positions. This behavior is described by the subsequent equations:

$$A = |C \cdot D(t - 1) - D(t - 1)| \tag{9}$$

$$D(t) = D(t - 1) \cdot \sin(2\Pi\Pi) - K \cdot A \tag{10}$$

where DE presents the vector toward the solution; DE is the position vector with the best solution globally in the t^{th} iteration with coefficient vectors CE and KE . DE changes the impact progress on the circle. To create a plume, each dolphin rapidly wiggles its tail in a

periodic manner similar to a sign, while the other dolphins circle the prey. The vector CE is calculated as follows in Equation (11):

$$C = 2 \cdot r \tag{11}$$

Any place in the search region may be reached by figuring out the random vector rE . Equation (5) replicates the prey being surrounded in this way, enabling any dolphin to defend its location near its present optimal position.

A population of random solutions is where the MRA search process begins (positions of dolphins). The dolphins defend their places in relation to either the best position found thus far or a dolphin chosen at random at each time step. As a result, a parameter is dependent on the transitional period between exploration and exploitation.

2.2. MRA-Based MPPT Technique

By altering the terminal voltages, the maximum power point of a multi-modular TEG power source with a centralized MPPT control scheme is monitored. At MPP, the terminal voltage is changed so that the power may be delivered to the load more effectively using a DC–DC converter (boost). To change the output voltages and achieve MPP, the duty cycle of the boost converter can be changed. This modification of the control action is carried out by an intelligent controller built on the MRA. The duty cycle is between 0 and 1.

The MPP tracking is performed by generating the reference voltage as Figure 5. The process is randomly initialized by four random duty cycles depicted by D1, D2, D3, and D4. Any large voltage fluctuation is caused by the abandonment of the least performing duty cycle, as D1 discovered at 0.01 s as a result of D2’s effect on the greater fitness score. D2 is detained for 0.09 s while search agent D4 successfully completes the GMPP. Within 200 ms, the remaining population has already begun to swiftly concentrate around D4. The voltage transients and power variations first exhibit extremely explorative activity.

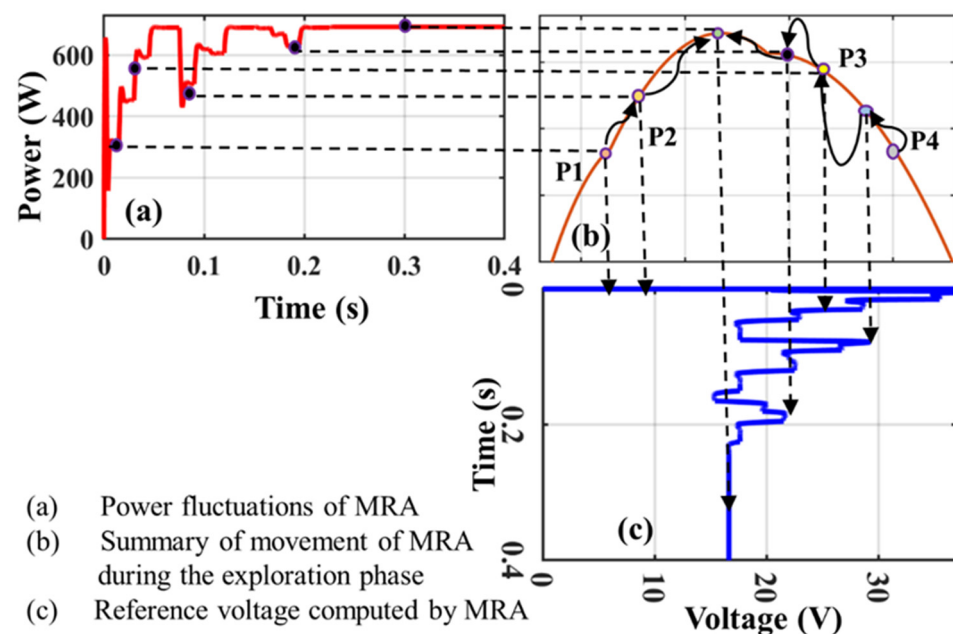


Figure 5. Tracking mechanism of MRA in TEG.

The population size is one of the most important aspects that must be properly tuned when adjusting the meta-heuristic optimization algorithm’s parameters. Low efficiency, sluggish convergence, and reduced volatility are caused by smaller populations. The exploratory behavior is maximized by using more particles, but the setup time is extended by the longer computing time. Therefore, there must be a careful balance between the

setting time and power tracking efficiency. As a result, $D_n = 4$ is selected for this study. The effectiveness of tweaking this parameter is examined with various population sizes.

The MRA procedure for MPPT is shown using a flowchart in Figure 6 as an example of an engineering problem for the TEG system.

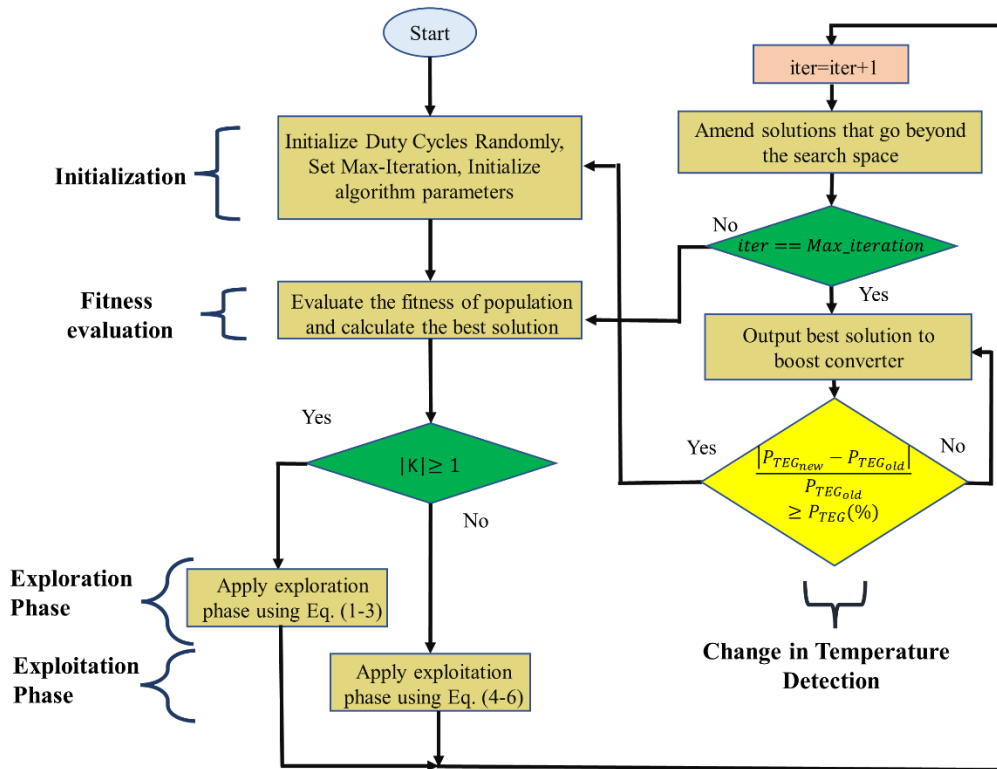


Figure 6. Flow chart of MRA.

Effective MPPT control requires the proper tuning of parameters to follow the global maxima. The sensitivity analysis is performed to determine the optimal parameter ranges. Poor parameter tuning leads to power loss as MPPT control fails to track the GMPP. The PSO algorithms experience fluctuations and oscillations from randomized location and velocity vectors, thus hindering the steady convergence to the global maximum power point (GMPP). The proposed method reduces the random variables, leading to fewer oscillations and higher energy production. Despite these challenges, the method effectively controls the TEG systems using MPPT.

2.3. Tracking Mechanism

Figure 5 shows the locations of the seeking particle in the search area using a tracking model for MRO. The duty cycle serves as the search space, and its range is from 0 to 1. Computing and contrasting each particle’s voltages avoids the need to repeatedly explore the search space. Four particles, $Pmr_1, Pmr_2, Pmr_3,$ and Pmr_4 , are initialized. The searching range of the voltage (min, max) by particle Pa_i ($i = 1, 2, \dots N$) is stored in the variable V_{Pa_i} . Equation (12) explains the selection of the best particle in terms of the voltage sample values of each particle:

$$V_{Pa_best(n)} = gbest(V_{Pa_best(1)}, V_{Pa_best(2)}, V_{Pa_best(3)}, V_{Pa_best(4)}) \tag{12}$$

The MRA-based MPPT controllers in Figure 5 compute a reference voltage from the duty cycle (c). In Figure 5, the equivalent power is displayed (a). Voltage surges are seen when a poor solution is abruptly dropped. The first stage of the optimization procedure is when this behavior is particularly prevalent. After 200 ms, the voltage transient becomes

stable. The GM is successfully tracked. A flow chart for the MRA-based MPPT is presented in Figure 6.

3. Results and Discussion

The MRA-based MPPT technique is cross examined in this section. The use of various case situations, including start-up tests, MPPT rating, widely fluctuating temperatures, statistical analysis, and an industrial environment with 24 h stochastic temperature profiling is followed by a hardware emulator experiment. Using a low-cost TEG emulation experimental setup, the performance of the suggested approach is validated in the actual world. A comparison is provided between the MRA-based MPPT control and other popular MPPT methods including the PSO, GWO, and WOA. The maximum number of iterations for meta-heuristic approaches is four, and their population size is four.

3.1. Start-Up Test:

The start-up test, which represents the TEG system’s zero point under non-NTD circumstances, is used to evaluate the MPPT approaches. In this instance, all strings had hot-side temperatures of 238 °C, 171 °C, 121 °C, and 81 °C, respectively, and cold-side temperatures of 52 °C, 45 °C, 23 °C, and 21 °C. Figure 7a,b compare power and duty cycles, respectively, demonstrating that the MRA adopts to the GM in the fewest iterations attaining the highest tracking efficiency in terms of the power magnitude with negligible oscillations at the GM.

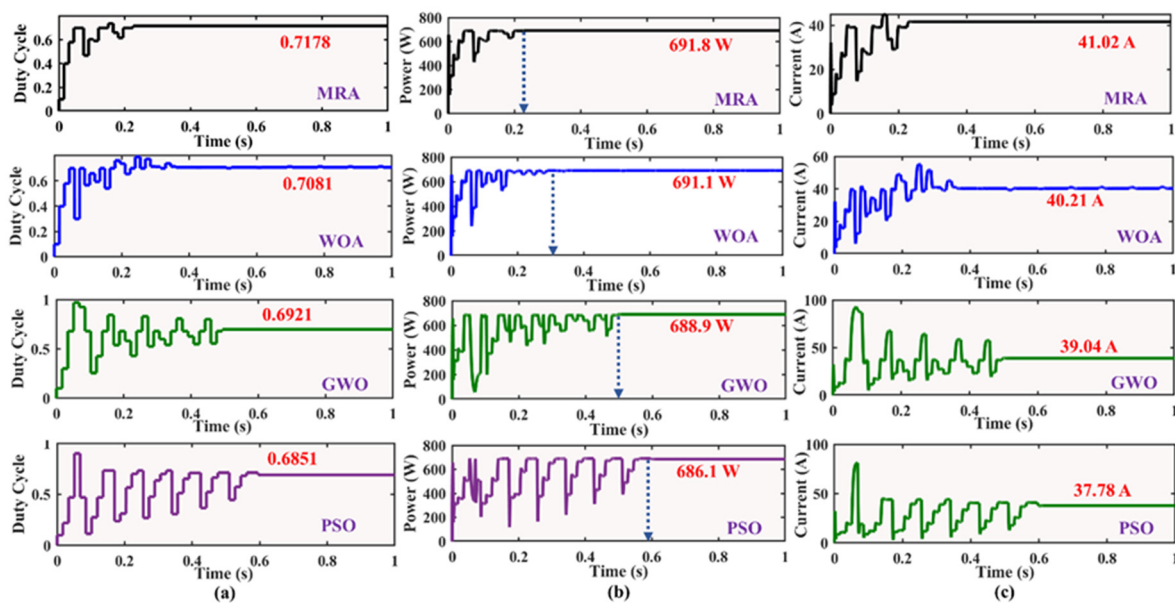


Figure 7. Comparative analysis of all techniques for Case 1 (a) Duty Cycle Variation (b) Power Tracking (c) Current Variation.

The large oscillations in the developed PSO may be seen in Figure 7. While these oscillations are also present in GWO because of the random probability selection function, which is used to avoid the LM traps, these periodically increasing oscillations are also present. The monitored powers by the MRA, WOA, GWO, and PSO are shown in Table 1 to be 691.8 W, 691.1 W, 688.9 W, and 686.1 W, respectively, with efficiency values of 99.97%, 99.86%, 99.55%, and 99.14%. Figure 7 confirms that the MRA tracks and settles at the GM in 220.2 ms, which is 80 ms–360 ms quicker than the WOA, GWO, and PSO. Figure 7b shows a comparison of the voltage transients. Energy extraction is another crucial criterion for comparison, and Table 2 and Figure 8 demonstrate that, when compared to other MPPT systems, MRA MPPT outclasses them in energy extraction.

Table 1. Comparative analysis for Case 1.

Tech.	Power Achieved (W)	Actual Global Power (W)	Efficiency (%)	Energy (W.s)	Tracking Time (s)
MRA	691.8	692	99.97	673.7	0.22
WOA	691.1	692	99.86	669.1	0.34
GWO	688.9	692	99.55	622.3	0.49
PSO	686.1	692	99.14	608.3	0.58

Table 2. Comparative analysis for Case 2.

Tech.	Power Achieved (W)	Actual Global Power (W)	Efficiency (%)	Energy (W.s)	Tracking Time (s)
MRA	404.35	404.5	99.96	1583	0.24
WOA	404	404.5	99.87	1570	0.36
GWO	403.45	404.5	99.74	1517	0.50
PSO	403.35	404.5	99.71	1513	0.61

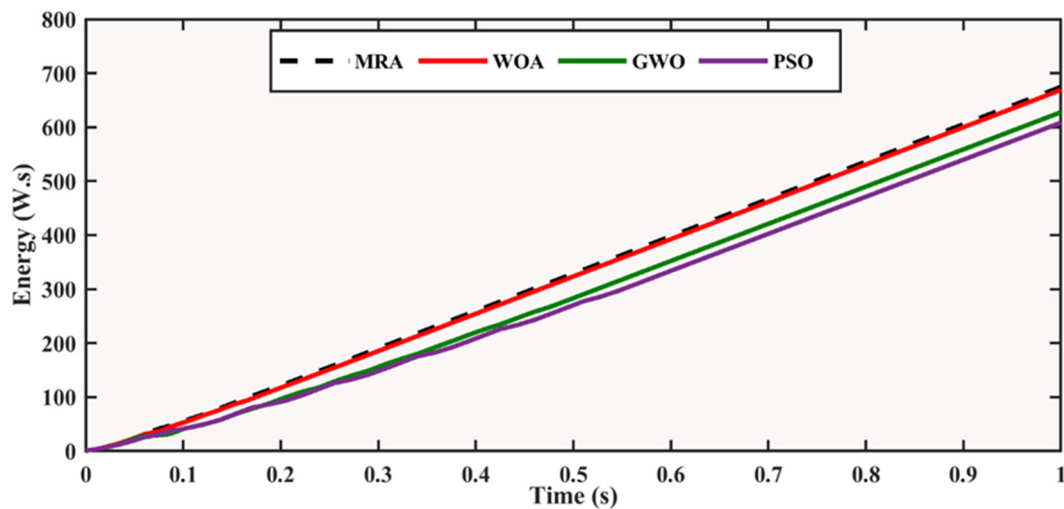


Figure 8. Energy comparison Case 1.

3.2. Varying Temperature

In this scenario, the cold-side temperature is held constant while the hot-side temperature quickly changes, causing a simultaneous NTD situation as shown in Figure 9, thus testing the durability of the MPPT approaches. Every two seconds, the temperature changes. The comparison is presented in Table 2.

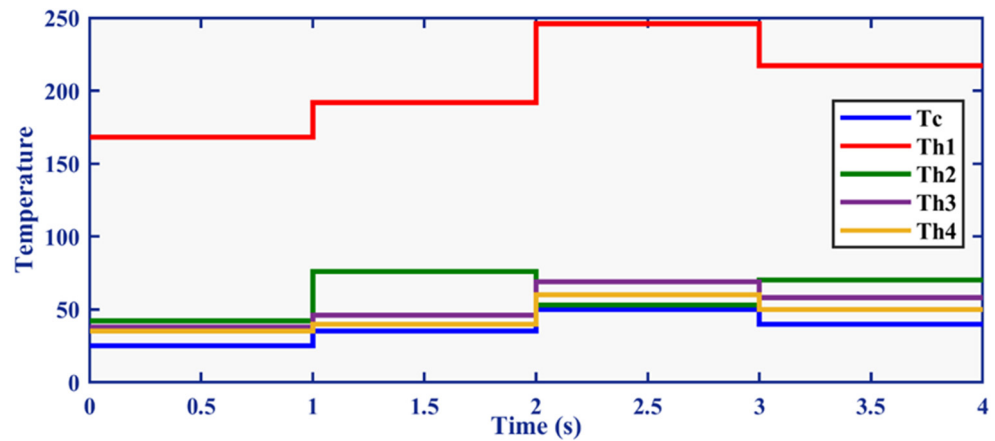


Figure 9. Temperature variation in Case 2.

Due to temperature variations, every meta-heuristic approach exhibits re-initialization, exploratory, and exploitative behavior after every two seconds Figure 10a. The MRA monitors the GM more quickly than the previous MPPT approaches and exhibits extremely low oscillations. The MRA, WOA, GWO, and PSO monitor the average power at 404.35 W, 404.0 W, 403.45 W, and 403.35 W, respectively. This demonstrates that the MRA tracks the biggest power loss due to significant oscillations at the GM. In this instance, the tracking efficiency is 99.96%, 99.87%, 99.74%, and 99.71%, respectively.

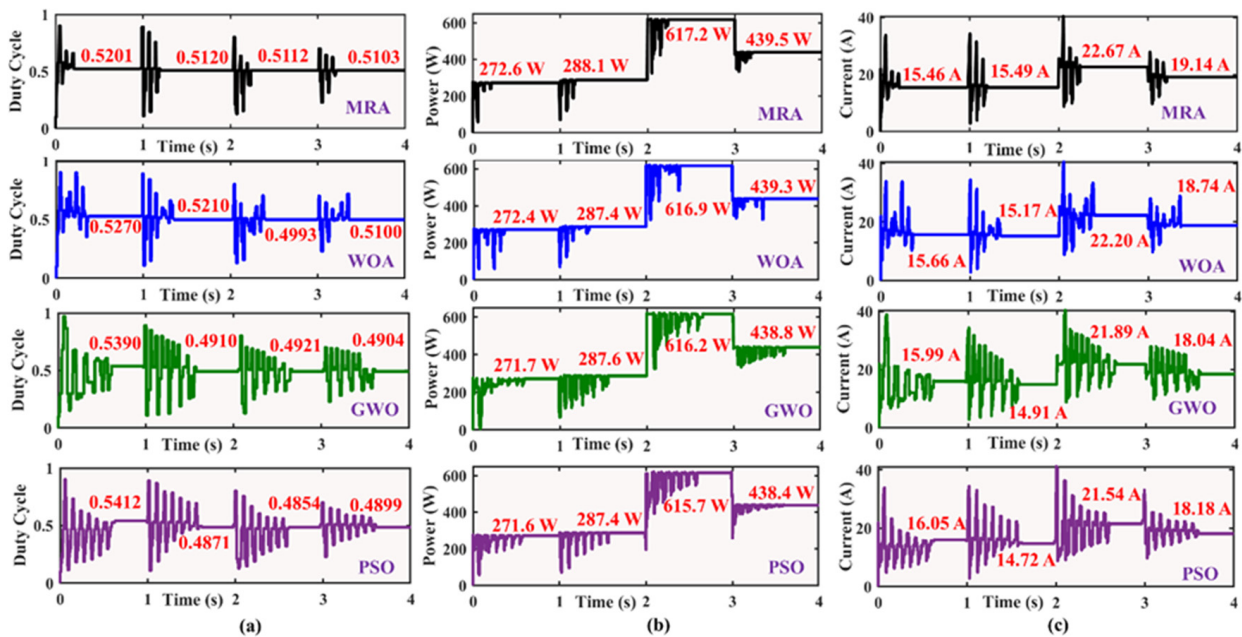


Figure 10. Comparative analysis of all techniques for Case 2 (a) Duty Cycle Variation (b) Power Tracking (c) Current Variation.

The track and settle times following the temperature change may be used to test the robustness of the MRA-based MPPT approach. According to Figure 10b, the average tracking times for the GM using the MPPT approaches are 240.1 ms, 360.3 ms, 500.2 ms, and 610.8 ms (b). Due to the dynamic population grouping that must be chosen each time, the WOA also requires a lot of time to track the GM. Due to this impact, the exploration is more time consuming. Figures 10c and 11 depict voltage transients and energy harvesting, respectively.

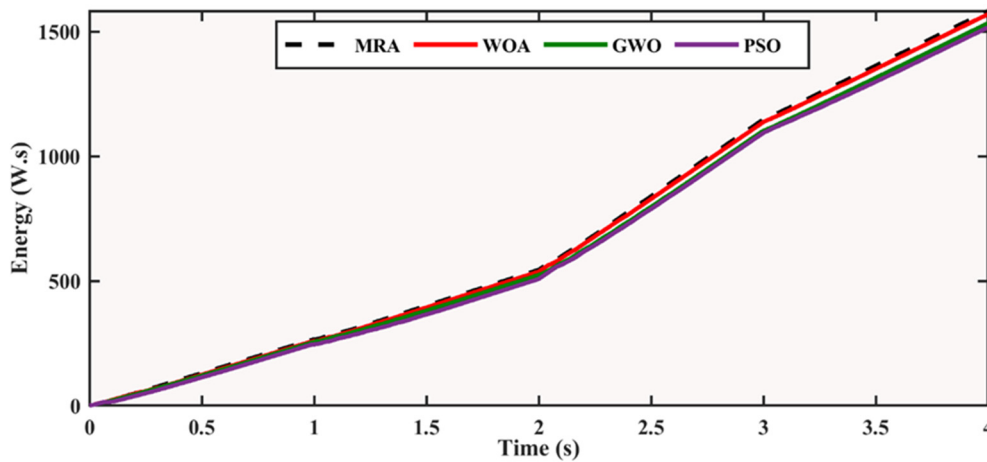


Figure 11. Energy comparison Case 2.

3.3. MPPT Rating

The MPPT rating is computed in this section using Equation (13). The variables for the ratings are: tuning parameter quantity (1–5), random numbers in algorithm (1–5), $iter_{max}$ for the GM location (1–5), tracking time (s), the efficiency (%age), the amount of hardware modification necessary for implementation, and the responsiveness of change in irradiance. The criteria for the selection of the ratings are shown in Figure 12. The criteria of the given values against every variable are shown in Equation (13).

$$MPPT_rating = \frac{Total\ achieved\ rating}{7} \tag{13}$$

<p>1 Tuning Parameter</p> <ul style="list-style-type: none"> Tuning Parameter=1; MPPT Rating=1; Tuning Parameter=2; MPPT Rating=2; Tuning Parameter=3; MPPT Rating=3; Tuning Parameter >=4; MPPT Rating=4; 	<p>2 Random Numbers</p> <ul style="list-style-type: none"> Random Numbers =0; MPPT Rating=1; Random Numbers =1; MPPT Rating=2; Random Numbers =2; MPPT Rating=3; Random Numbers >=3; MPPT Rating=4; 	<p>3 Termination Criteria Met?</p> <ul style="list-style-type: none"> Termination Criteria Met = Yes MPPT Rating=2; Termination Criteria Met = No MPPT Rating=1;
<p>4 Average Tracking Time</p> <ul style="list-style-type: none"> Tracking Time=0-500ms; MPPT Rating=1; Tracking Time=500-750ms; MPPT Rating=2; Tracking Time=750-1000ms; MPPT Rating=3; Tracking Time >=1000ms; MPPT Rating=4; 	<p>5 MPPT Percentage Efficiency</p> <ul style="list-style-type: none"> MPPT Efficiency=99.5-100% MPPT Rating=1; MPPT Efficiency=99-99.5% MPPT Rating=2; MPPT Efficiency=98.5-99% MPPT Rating=3; MPPT Efficiency >=98.5% MPPT Rating=4; 	
<p>6 Hardware Modification Required?</p> <ul style="list-style-type: none"> Hardware Modification= Yes MPPT Rating=2; Hardware Modification = No MPPT Rating=1; 	<p>7 Response Time to Variation</p> <ul style="list-style-type: none"> Response Time >=0.25s MPPT Rating=1; Response Time =0.25-0.50s MPPT Rating=2; Response Time =0.50-0.75s MPPT Rating=3; Response Time >=0.75s MPPT Rating=4; 	

Figure 12. MPPT rating criteria in figure form.

According to Table 3, the MRA does have the greatest MPPT rating of 1.285, indicating that it can follow the GM significantly more quickly. MPPT implementation for the MRA is straightforward because only one tuning parameter is needed. Because the MRA uses only

one random number, the oscillations are also reduced. A graphical representation of the MPPT rating achieved by the competing techniques is shown in Figure 13.

Table 3. MPPT rating comparison.

Tech. Name	Tuning Parameter Number	Rand. No.	Termination Criteria Achieved?	Avg. TT (s)	Avg. Effic. (%)	Hardware Modification	Response Time in Variation (s)	Rating Score
MRA	1 (1)	2 (2)	No (1)	0.23 (1)	99.96 (1)	No (1)	Fast (2)	1.285
WOA	3 (3)	1 (1)	Yes (2)	0.35 (1)	99.86 (1)	Yes (2)	Slow (3)	1.857
GWO	2 (2)	2 (3)	Yes (2)	0.49 (1)	99.65 (1)	No (1)	Very slow (4)	2.000
PSO	3 (3)	2 (3)	Yes (2)	0.60 (2)	99.42 (2)	No (1)	Very slow (4)	2.423

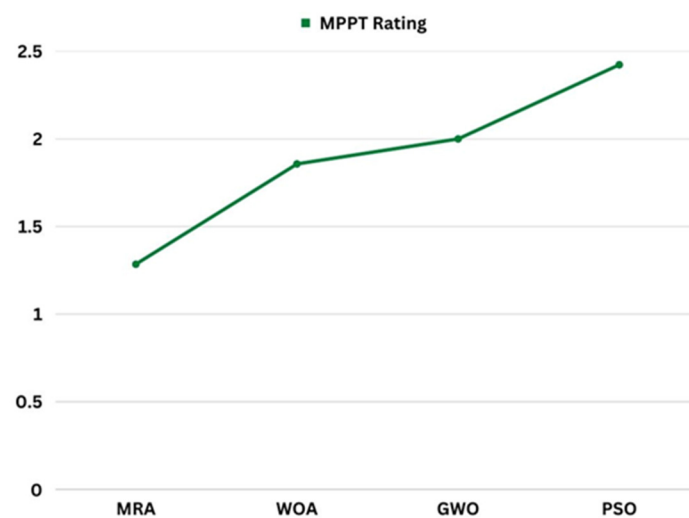


Figure 13. Graphical representation of MPPT rating.

The traditional gradient-based MPPT approaches are prone to power loss due to their inability to follow the GM under NUT. The metaheuristic approaches, i.e., the WOA and PSO, are a good way to deal with it, but the oscillations at the GM and extended tracking times lead to persistent oscillations that accumulate into a loss of power and efficiency. The MRA's effective behavior fixes the aforementioned issues and effectively tracks the GM up to 99.95% of the time. Additionally, the MRA tracks the GM up to 341.1 ms, which is 53.9% quicker than PSO. Because of this MRA capacity, the GM oscillations are extremely low and attain significant energy in comparison. Energy is extracted from the thermoelectric generator system 5.2% greater by the MRA. The current and voltage oscillations and variations are likewise less pronounced in the MRA. To fulfil the stopping requirements, the MRA uses a maximum of 18 iterations. The MRA obtains a superior MPPT rating because it uses fewer tuning parameters and random numbers.

3.4. Experimental Results

TEG systems are extremely risky and challenging to work with in real-time applications. Using an equivalent model to the TEG emulator described in Section 2, an emulator circuit is designed. TEG is a temperature-dependent voltage source whose open-circuit voltage (V_{oc}) varies with the temperature difference. To simulate the internal resistance (R_{TEG}) of a TEG module, a power source with a high wattage and low resistance is connected in series. To simulate the temperature changes, a rapid-voltage-changing DC source is altered by shorting the diode array. Figure 14 depicts the connections between the electrical components. Table 4 lists the parts that were utilized to establish the MPPT control for the TEG system. In addition to the limitations, the sensor noise sensitivity in the measurement

also affects the MPPT control performance by causing fluctuations in the control system. To overcome these limitations and achieve satisfactory performance in MPPT control, careful design and implementation of the Mud Ring Optimization (MRO) algorithm is crucial. This study contributes to the advancement of the MPPT control for TEG systems and the implementation of renewable energy technologies. The MRO algorithm demonstrates exceptional performance in dynamic thermal environments, tracking the maximum power point with a higher efficiency than conventional MPPT methods. The experimental results again show an average power output of 99.95% and faster response time of 220 ms, thus resulting in the faster tracking of the global maximum power point (GM) under dynamic conditions, with an improvement of up to 70% less tracking time.

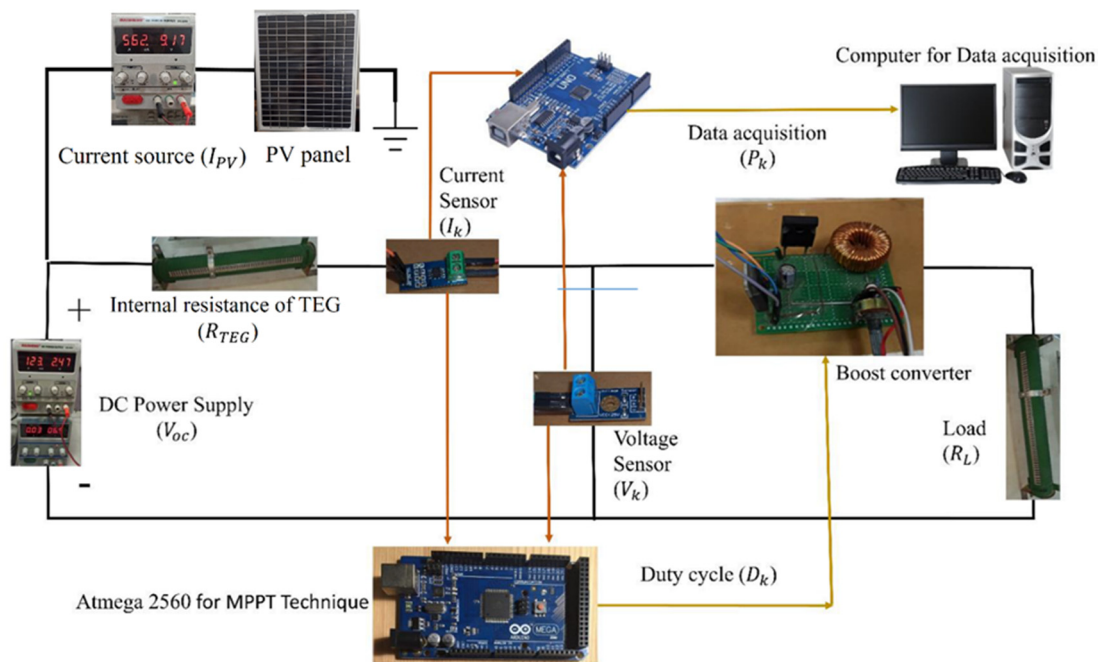


Figure 14. Hardware setup figure.

Table 4. The electrical characteristics of hardware modules.

Component	Magnitude
Current at MPP (I_{max})	1.0702 A
Ideality factor	1.0037
Maximum power (P_{max})	20.1 W
Peak efficiency	19.3%
Open circuit voltage (V_{oc})	22.7 V
Series resistance R_s	1.0547 Ω
Short circuit current (I_{sc})	1.17 A
Shunt resistance R_{sh}	405.96 Ω
Temperature coefficient of I_{sc}	0.043%/K
Temperature coefficient of V_{oc}	-0.35%/K
Voltage at MPP (V_{max})	18.76 V

MRA has a powerful reaction with effective completion well within 200 ms, which contrasts GWO and PSO. Lower time, less oscillations, and excellent efficiency are all achieved using the MRA. Figure 15 demonstrates the power tracked by the MRA. The

GWO has a different foraging strategy and exhibits a marginal improvement in settling time, requiring 350. The results demonstrate the constraining mathematical model that aids GWO control action by reducing the rapid fluctuations; however, the probabilistic selection of weak solutions for maximal search space exploitation constrains the quicker settling time. The PSO's power tracking is displayed in Figure 15, where 400 ms is used. Low waves are seen after settling at the GM, as seen in the zoomed-in picture. With less effective control action, less power is generated, increasing the power loss. The experimental data cause the impact of the exploratory, hybrid, and exploitative phases to be very evident. In the MRA, strong exploration behavior is shown in the beginning of the iterations, and, after a few iterations, few particles start exploitation, which reduces the oscillations. The exploitation begins at the conclusion of the iterative procedure, causing the MRA to settle at the GM without oscillations. The experimental findings support the MRA's better performance in all the testing configurations.

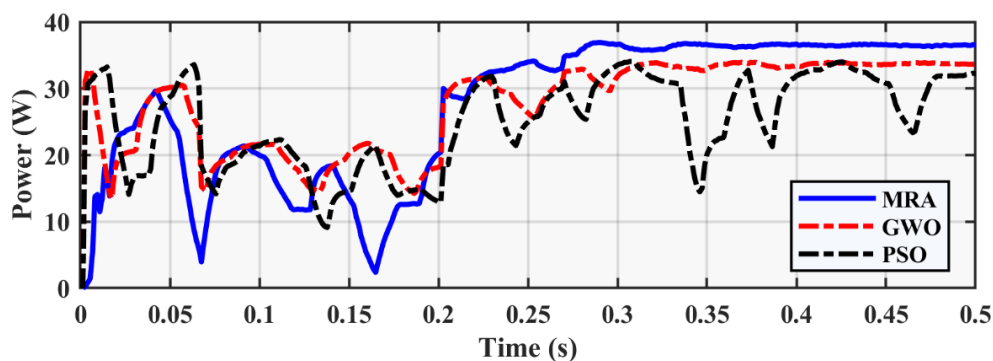


Figure 15. PSO, GWO, and MRA hardware results.

4. Conclusions

In this paper, a novel MRA-based MPPT control approach is developed using a low-cost microcontroller to considerably reuse the waste heat that is produced during the industrial process. A detailed modeling of the TEG system, MRA algorithm, and operating conditions was performed. The results are compared to the well-established stochastic algorithms GWO, WOA, and PSO. The MRA is compared to other meta-heuristic methods in terms of the tracking time, energy harvest, % age power tracking efficiency, MPPT rating, and hardware experimental emulator setup. The MRA demonstrates superior performance. The MRA settle at the GM with improved efficiency of up to 99.95% and less than 38–70% faster tracking times. To verify the MPPT control's capacity to converge and its resilience, the MRA is put through a variety of tests. The MRA is evaluated on a low-cost TEG emulator and implemented on a low-cost microcontroller, demonstrating the higher performance of the suggested MPPT control approach. This provides enough evidence for a practical application of the MRA as a cost effective MPPT control of a centralized TEG system in an industrial environment.

- The MRA-based MPPT technique tracks the GMPP under NUTD with 99.96% efficiency within 220 ms.
- The strong capability to differentiate between the LMPP and GMPP with an improvement of up to 70% lesser tracking time.
- The experimental verification is achieved on a low-cost microcontroller, thus facilitating large-scale adoption in existing and new MPPT applications.

In future, large-scale TEG shall be studied with an AC grid using inverter topologies to gauge the impact of the TEG system as a heat recovery unit in the rotary kiln of a 10,000 TPD cement plant.

Author Contributions: Data curation, Resources, Writing—original draft, Visualization, M.H.Z.; Formal analysis, Methodology, Writing—review & editing, M.A.H.; Investigation, M.M.; Methodology, Validation, N.M.K.; Investigation, Writing—original draft, S.K.R.M.; Software, Resources, Visualization, M.K.K.; Project administration, Funding acquisition, Supervision, N.A. All authors have read and agreed to the published version of the manuscript.

Funding: This research received no external funding.

Institutional Review Board Statement: Not Applicable.

Informed Consent Statement: Not Applicable.

Data Availability Statement: No data is used in this study.

Conflicts of Interest: The Authors declare no conflict of interest.

Abbreviations

TEG	Thermoelectric Generator;
MPPT	Maximum Power Point Tracking;
P&O	Perturb and Observe;
IC	Incremental Conductance;
MRA	Mud Ring Optimizer;
GWO	Grey Wolf Optimizer;
GM	Global Maxima;
PSO	Particle Swarm Optimization;
WOA	Whale Optimization Algorithm;
GMPP	Global Maximum Power Point;
LMPP	Local Maximum Power Point.

References

1. Khan, M.K.; Zafar, M.H.; Mansoor, M.; Mirza, A.F.; Khan, U.A.; Khan, N.M. Green energy extraction for sustainable development: A novel MPPT technique for hybrid PV-TEG system. *Sustain. Energy Technol. Assess.* **2022**, *53*, 102388.
2. Zafar, M.H.; Khan, N.M.; Mirza, A.F.; Mansoor, M.; Akhtar, N.; Qadir, M.U.; Khan, N.A.; Moosavi, S.K.R. A novel meta-heuristic optimization algorithm based MPPT control technique for PV systems under complex partial shading condition. *Sustain. Energy Technol. Assess.* **2021**, *47*, 101367.
3. Bollipo, R.B.; Mikkili, S.; Bonthagorla, P. Critical Review on PV MPPT Techniques: Classical, Intelligent and Optimisation. *IET Renew. Power Gener.* **2020**, *14*, 1433–1452. [[CrossRef](#)]
4. Aoughlis, C.; Belkaid, A.; Colak, I.; Guenounou, O.; Kacimi, M.A. Automatic and Self Adaptive P&O MPPT Based PID Controller and PSO Algorithm. In Proceedings of the 2021 10th International Conference on Renewable Energy Research and Application (ICRERA), Istanbul, Turkey, 26–29 September 2021.
5. Renaudineau, H.; Donatantonio, F.; Fontchastagner, J.; Petrone, G.; Spagnuolo, G.; Martin, J.-P.; Pierfederici, S. A PSO-based global MPPT technique for distributed PV power generation. *IEEE Trans. Ind. Electron.* **2014**, *62*, 1047–1058. [[CrossRef](#)]
6. Ishaque, K.; Salam, Z.; Amjad, M.; Mekhilef, S. An improved particle swarm optimization (PSO)-based MPPT for PV with reduced steady-state oscillation. *IEEE Trans. Power Electron.* **2012**, *27*, 3627–3638. [[CrossRef](#)]
7. Mohanty, S.; Subudhi, B.; Ray, P. A new MPPT design using grey wolf optimization technique for photovoltaic system under partial shading conditions. *IEEE Trans. Sustain. Energy* **2015**, *7*, 181–188. [[CrossRef](#)]
8. Mansoor, M.; Mirza, A.; Ling, Q. Harris hawk optimization-based MPPT control for PV Systems under Partial Shading Conditions. *J. Clean. Prod.* **2020**, *274*, 122857. [[CrossRef](#)]
9. Mansoor, M.; Mirza, A.F.; Ling, Q.; Javed, M.Y. Novel Grass Hopper optimization based MPPT of PV systems for complex partial shading conditions. *Sol. Energy* **2020**, *198*, 499–518. [[CrossRef](#)]
10. Jiang, L.L.; Maskell, D.; Patra, J. A novel ant colony optimization-based maximum power point tracking for photovoltaic systems under partially shaded conditions. *Energy Build.* **2013**, *58*, 227–236. [[CrossRef](#)]
11. Kinattungal, S.; Simon, S.; Nayak, P. MPPT in PV systems using ant colony optimisation with dwindling population. *IET Renew. Power Gener.* **2020**, *14*, 1105–1112.
12. Lyden, S.; Haque, M. A simulated annealing global maximum power point tracking approach for PV modules under partial shading conditions. *IEEE Trans. Power Electron.* **2015**, *31*, 4171–4181. [[CrossRef](#)]
13. Ahmed, J.; Salam, Z. A Maximum Power Point Tracking (MPPT) for PV system using Cuckoo Search with partial shading capability. *Appl. Energy* **2014**, *119*, 118–130. [[CrossRef](#)]
14. Ma, J.; Ting, T.O.; Man, K.L.; Zhang, N.; Guan, S.-U.; Wong, P.W.H. Parameter estimation of photovoltaic models via cuckoo search. *J. Appl. Math.* **2013**, *2013*, 362619. [[CrossRef](#)]

15. Li, H.; Yang, D.; Su, W.; Lu, J.; Yu, X. An overall distribution particle swarm optimization MPPT algorithm for photovoltaic system under partial shading. *IEEE Trans. Ind. Electron.* **2018**, *66*, 265–275. [[CrossRef](#)]
16. Mirza, A.F.; Ling, Q.; Javed, M.Y.; Mansoor, M. Novel MPPT techniques for photovoltaic systems under uniform irradiance and Partial shading. *Sol. Energy* **2019**, *184*, 628–648. [[CrossRef](#)]
17. Agwa, A.M.; El-Fergany, A.; Maksoud, H. Electrical characterization of photovoltaic modules using farmland fertility optimizer. *Energy Convers. Manag.* **2020**, *217*, 112990. [[CrossRef](#)]
18. Huang, C.; Wang, L.; Yeung, R.S.-C.; Zhang, Z.; Chung, H.S.-H.; Bensoussan, A. A prediction model-guided Jaya algorithm for the PV system maximum power point tracking. *IEEE Trans. Sustain. Energy* **2017**, *9*, 45–55. [[CrossRef](#)]
19. Mirza, A.F.; Mansoor, M.; Ling, Q.; Yin, B.; Javed, M.Y. A Salp-Swarm Optimization based MPPT technique for harvesting maximum energy from PV systems under partial shading conditions. *Energy Convers. Manag.* **2020**, *209*, 112625. [[CrossRef](#)]
20. Fathy, A. Butterfly optimization algorithm based methodology for enhancing the shaded photovoltaic array extracted power via reconfiguration process. *Energy Convers. Manag.* **2020**, *220*, 113115. [[CrossRef](#)]
21. Soufyane Benyoucef, A.; Chouder, A.; Kara, K.; Silvestre, S.; Sahed, O.A. Artificial bee colony based algorithm for maximum power point tracking (MPPT) for PV systems operating under partial shaded conditions. *Appl. Soft Comput.* **2015**, *32*, 38–48. [[CrossRef](#)]
22. Zhao, Z.; Cheng, R.; Yan, B.; Zhang, J.; Zhang, Z.; Zhang, M.; Lai, L.L. A dynamic particles MPPT method for photovoltaic systems under partial shading conditions. *Energy Convers. Manag.* **2020**, *220*, 113070. [[CrossRef](#)]
23. Zhang, R.; Yang, B.; Chen, N. Arithmetic optimization algorithm based MPPT technique for centralized TEG systems under different temperature gradients. *Energy Rep.* **2022**, *8*, 2424–2433. [[CrossRef](#)]
24. Priyadarshi, N.; Ramachandaramurthy, V.; Padmanaban, S.; Azam, F. An ant colony optimized MPPT for standalone hybrid PV-wind power system with single Cuk converter. *Energies* **2019**, *12*, 167. [[CrossRef](#)]
25. Abdullah, J.M.; Ahmed, T. Fitness dependent optimizer: Inspired by the bee swarming reproductive process. *IEEE Access* **2019**, *7*, 43473–43486. [[CrossRef](#)]
26. Mansoor, M.; Mirza, A.F.; Long, F.; Ling, Q. An Intelligent Tunicate Swarm Algorithm Based MPPT Control Strategy for Multiple Configurations of PV Systems Under Partial Shading Conditions. *Adv. Theory Simul.* **2021**, *4*, 2100246. [[CrossRef](#)]
27. Maher, R.A.; Abdelsalam, A.K.; Dessouky, Y.G.; Nouman, A. High performance state-flow based MPPT technique for micro WECS. *IET Renew. Power Gener.* **2019**, *13*, 3009–3021. [[CrossRef](#)]
28. Tatabhatla, V.M.R.; Agarwal, A.; Kanumuri, T. Improved power generation by dispersing the uniform and non-uniform partial shades in solar photovoltaic array. *Energy Convers. Manag.* **2019**, *197*, 111825. [[CrossRef](#)]
29. Lasheen, M.; Rahman, A.K.A.; Abdel-Salam, M.; Ookawara, S. Adaptive reference voltage-based MPPT technique for PV applications. *IET Renew. Power Gener.* **2017**, *11*, 715–722. [[CrossRef](#)]

Disclaimer/Publisher’s Note: The statements, opinions and data contained in all publications are solely those of the individual author(s) and contributor(s) and not of MDPI and/or the editor(s). MDPI and/or the editor(s) disclaim responsibility for any injury to people or property resulting from any ideas, methods, instructions or products referred to in the content.